Performance assessment of electro-osmotic flow of rectangular microchannels with smoothed corners

Performance assessment of electro-osmotic flow of rectangular microchannels with smoothed corners

Nicola Suzzi[1] **and Marco Lorenzini**[2]

[1]Dipartimento Politecnico di Ingegneria e Architettura - Università di Udine - Via delle Scienze - 33100 - Udine (UD) - Italy
[2]Dipartimento di Ingegneria Industriale, Campus di Forlì - Università di Bologna - Via Fontanelle 40 - 47121 Forlì (FC) - Italy

E-mail: marco.lorenzini@unibo.it

Abstract. Microchannel heat sinks are a viable alternative to traditional thermal management systems when high fluxes over small surfaces are involved. To avoid high pressure drops especially when liquids are concerned, electro-osmotic flow, a phenomenon which is relevant at the microscales only, can be employed profitably. Joule heating, which occurs every time an electrical current is circulated through a conductor with finite electrical resistance, may hamper the application of electro-osmotic flows significantly; its effects must therefore be investigated, as should the influence of the entry length on the overall transport phenomena which occur in the microchannel, especially so since channels with uniform temperature at the walls tend to be somewhat short, to mitigate heat generation due to Joule heating. In this paper the transport phenomena occurring within a microchannel of rectangular cross-section with uniform wall temperature through which an electro-osmotic flow occurs is studied, while considering the flow fully developed hydrodynamically but thermally developing (Graetz problem). The corners are then smoothed progressively and the effect of this change in the shape of the cross-section over the non-dimensional dissipated power or temperature difference between wall and fluid is investigated using the performance evaluation criteria introduced by Webb. Correlations are suggested for the Poiseuille and Nusselt numbers for all configurations as are criteria to obtain the maximum allowable channel length, i.e. the length of the channel over which the walls start to cool the fluid, owing to Joule heating, in terms of the hydraulic diameter.

1. Introduction

Research on microchannels has been a lively field for the past thirty years or so, owing to the compactness associated with mirco-flow devices (MFDs)and to the exploitability of physical effects relevant at the microscale only, [1, 2]. Research on fundamental issues is still ongoing, [3–7], but MFDs have found application in a number of fields, and the future also seems quite promising, [8–10]. One such field is the thermal management of electronic devices, since microchannel heat sinks are able to remove high heat fluxes, owing to the high heat transfer coefficients involved, albeit at the expenses of high pressure drops, which may become exceedingly large, especially when liquids are involved. One possible solution is offered by a physical phenomenon which is significant at the microscale only, namely electro-osmosis, which allows motion of a liquid relative to a charged surface, when an external electric field is applied across a microchannel [11]. If the channel walls have a net electrical charge and the channel is filled with a polar fluid, an inhomogeneous charge distribution develops in the liquid; if an external electric field is then applied, its action on the layer of mobile ions close to the walls generates a flow, which is called electro-osmotic (EOF). No moving parts are present in EOF devices, which have no issues related to

noise or vibrations, and no lubrication is needed at all. Given the dimensions involved, liquid reservoirs have minimal volumes and they can be directly bored/etched onto the silicon chips. Experiments on EOFs have reported Nusselt numbers 10% larger than than pressure-driven flow (PDFs) for the same geometry, yet the effect of Joule heating may become relevant when a certain threshold in the value of the applied electric field is reached, [12]. Further issues of EOF are the alteration in the velocity profiles which is caused by the chemical composition at the interface, and they are largely different from those which characterise pressure-driven flows, and the undesirable heat dissipation from Joule heating, which may partly or completely offset its cooling action, [11]. In the quest for increasing the heat transfer performance of electro-osmotic flows, several fundamental investigations on a variety of cross-sections were carried out, ranging from the common circular ducts and parallel plates [13], to unusual geometries such as polygonal, elliptical and triangular ducts, [14]. Similarly, the use of electro-osmotic pumps (EOPs) has been investigated, [12, 15, 16], sometimes with the specific purpose of electronics cooling, [12, 17]. One survey of the research carried out in the field evidences how the geometry of the channel is a subject occurring quite frequently, also thanks to the fast development in the manufacturing processes and technologies for micro-fabrication. In this context, one natural development is the shape optimisation of the cross-section, which can lead to an improvement in performance as measured by an increase in heat transfer and a decrease in pressure drop and entropy production. This can be achieved among others by smoothing the corners of the cross-section, as demonstrated in [18] for the case of laminar flow without viscous dissipation in ordinary ducts. The investigation was then extended to pressure-driven flows in microchannels with and without viscous dissipation, [19, 20], and to electro-osmotic flows in the fully developed and constant heat flux and perimeter temperature case [21], employing the results to carry out a first-law analysis based on performance evaluation criteria (PEC), [22], and on entropy production minimisation. Though it is often neglected in the analysis of transport phenomena in laminar flows within microchannels, the study of the thermal entry region of a hydrodynamically fully developed, flow, known as the Graetz problem, is a feature which may become dominant, as demonstrated for the case of non-negligible viscous dissipation, [23], and of electro-osmotic flows with uniform temperature over the channel walls, [24]. This work investigates the change in constrained heat transfer performance, expressed as the change in heat flux or temperature difference from a reference configuration (i.e. sharp corners) for a rectangular cross-section, in the case of EOF with Joule heating and uniform temperature boundary conditions. The Graetz problem solved in [24] provides the values of the Poiseuille and Nusselt numbers which are correlated to the operating and geometrical conditions. Optimisation is then carried out for the subset of PECs which the link between the thermophysical, electrical and geometrical quantities allows. The purpose is both to contribute to the fundamental understanding of the phenomena involved and to supply correlations of practical significance when designing such devices.

2. Mathematical model

The geometry investigated is that of rectangular channel whose corners are progressively smoothed, as shown in Figure 1, and is further discussed below. For the sake of compactness, only the non-dimensional forms of the governing equations are reported in the following, the reader is referred to [24], in particular the Appendix, and to [21] for how the equations are derived. All equations are written for a Cartesian reference system, with the z coordinate along the flow direction and the x and y coordinates referring to the cross-section, see Figure 1.

2.1. Energy balance under uniform temperature boundary condition

Consider a control volume within a channel, as the one shown in Figure 1, through which a fluid flows steadily, with constant cross section. The fluid is Newtonian, with constant thermo-physical properties, and the temperature at the wall is uniform over the whole channel. The flow is hydrodynamically developed, yet not thermally, and Joule heating occurs within it. The energy balance for a control volume

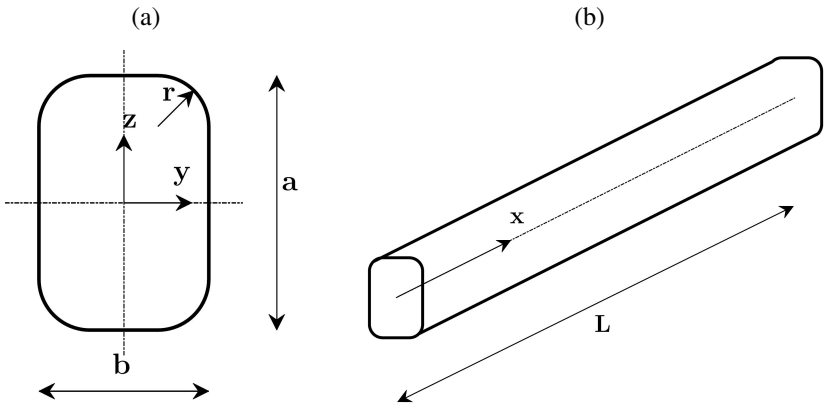

Figure 1. Reference Cartesian coordinate system: channel cross section geometry (a), channel axis (b).

within the channel yields,

$$\dot{m} c_p \frac{\mathrm{d}T_b}{\mathrm{d}x} = \alpha P \Delta T + \dot{q}_s A_c, \tag{1}$$

where $\dot{q}_s$ is the volumetric heat generation due to Joule heating; integration gives the difference, ΔT between the bulk and wall temperatures, T_b and T respectively, along the channel length:

$$\Delta T = \left(\Delta T_i + \frac{\dot{q}_s A_c}{\overline{\alpha} P} \right) \exp\left(-\frac{\overline{\alpha} P x}{\dot{m} c_p} \right) - \frac{\dot{q}_s A_c}{\overline{\alpha} P}. \tag{2}$$

The global heat flux can be derived from the calculated temperature profile, via integration of the local heat flux per unit length, $q' = \alpha P \Delta T$, along the channel:

$$q = \dot{m} c_p \Delta T_i \left(1 + \frac{\dot{q}_s A_c}{\overline{\alpha} P \Delta T_i} \right) \left[1 - \exp\left(-\frac{\overline{\alpha} P L}{\dot{m} c_p} \right) \right] - \dot{q}_s A_c L. \tag{3}$$

Introducing the following non-dimensional quantities,

$$q^* = \frac{q}{q_0}, \Delta T^* = \frac{\Delta T_i}{\Delta T_{i,0}}, \dot{m}^* = \frac{\dot{m}}{\dot{m}_0}, W* = \frac{W}{W_0}, L^* = \frac{L}{L_0}, A_c^* = \frac{A_c}{A_{c,0}}, P^* = \frac{P}{P_0}, \tag{4}$$

$$\eta = \frac{\overline{\alpha} P L}{\dot{m} c_p} = 4 \frac{\mathrm{Nu}}{\mathrm{Pe}} \frac{L}{D_h}, \xi = \frac{\dot{q}_s A_c L}{\dot{m} c_p \Delta T_i}, \tag{5}$$

with $\overline{\mathrm{Nu}} = \overline{\alpha} D_h / \lambda$ being the Nusselt number averaged over the whole channel length, $\mathrm{Pe} = \rho c_p u_b D_h / \lambda$ being the Peclet number and the subscript 0 denoting the reference configuration, Eq. (3) can be recast into non-dimensional form:

$$q^* = \frac{\dot{m}^* \Delta T^* \left(1 - e^{-\eta}\right) + \xi_0 \left(A_c^* L^*\right) \left(\frac{1 - e^{-\eta}}{\eta} - 1 \right)}{1 - e^{-\eta_0} + \xi_0 \left(\frac{1 - e^{-\eta_0}}{\eta_0} - 1 \right)}. \tag{6}$$

Depending on the applied PEC, Eq. (3) can be used to determine the actual heat flux q or the inlet temperature difference ΔT_i between solid wall and fluid bulk. However, we first need to estimate the mass flow rate $\dot{m}$, the effective channel length L and the average heat transfer coefficient $\overline{\alpha}$, in order to apply Eq. (3).

2.2. Electro-osmotic flow: governing equations

Both the flow and temperature fields of an electro-osmotic, thermally developing flow inside a channel, see Figure 1, under T boundary condition had been previously solved by the authors for several cases, [21, 24], in order to get pieces of information on the Poiseuille and Nusselt numbers, which are required by PEC based optimization of a microchannel geometry. To do so, the non-dimensional governing equations with the boundary conditions,

$$\frac{\partial^2\Psi}{\partial Y^2}+\frac{\partial^2\Psi}{\partial Z^2}=(k_D D_h)^2\sinh\Psi,\ \Psi|_{\partial\Omega}=\Psi_0, \tag{7}$$

$$\frac{\partial^2 U}{\partial Y^2}+\frac{\partial^2 U}{\partial Z^2}=E\sinh\Psi,\ U|_{\partial\Omega}=0, \tag{8}$$

$$\mathrm{Pe}\,\frac{U}{U_b}\frac{\partial\Theta}{\partial X}=\frac{\partial^2\Theta}{\partial Y^2}+\frac{\partial^2\Theta}{\partial Z^2}+Q,\ \Theta|_{\partial\Omega}=0, \tag{9}$$

were numerically solved via `bim` package, provided by the open source software `GNU Octave`, with the non-dimensional variables $\mathbf{X}$, Ψ, U and Θ being equal to:

$$\mathbf{X}=\frac{\mathbf{x}}{D_h},\ \Psi=\frac{z_i\,e\,\psi}{k_B\,T_w},\ U=\frac{\mu\,u}{\varepsilon\,\zeta\,E_x},\ \Theta=\frac{T-T_w}{T_i-T_w}. \tag{10}$$

In the expression of the non-dimensional electric potential in the fluid, Ψ, e is the elementary charge, z_i the ion valence, k_B Boltzmann's constant and *psi* the dimensional electric potential, whilst in the expression of the non-dimensional fluid velocity, U, μ is the fluid viscosity, ε the electrical permittivity, ζ the potential on the Stern plane and E_x the external electric field in dimensional form. The full explanation of the mathematical model with derivation of the governing equations, the discussion of the numerical method and the model validation are provided in [24]. Numerical verification of the model was carried out against the results in [21], whilst the experimental data provided by [12, 25] were used for its validation, see [24].

3. Problem statement

3.1. Performance Evaluation Criteria

Performance Evaluation Criteria (PEC) define a procedure for heat exchanger design based on the first law of thermodynamics. The objective functions of PEC are: global heat flux q, inlet temperature difference between solid wall and bulk fluid $\Delta T_i = T_w - T_i$, pumping power W, channel length L. Depending on the design requirements and, thus, on the applied PEC, we have to optimize one of the objective functions, while restrictions are applied to other quantities, as listed in Table 1, where acronyms FG and VG refer to fixed and variable geometry respectively, with the remaining characters denoting which quantities are optimised and under which constraints, [26].

Table 1. Performance Evaluation Criteria.

Criterion	q/q_0	$\Delta T/\Delta T_0$	$\dot{m}/\dot{m}_0$	W/W_0	L/L_0
FG1a	↑	1	1		1
FG1b	1	↓	1		1
FG2a	↑	1		1	1
FG2b	1	↓		1	1
VG2a	↑	1	1	1	
VG2b	1	↓	1	1	

Here, we focus on the geometrical optimization of a microchannel heat sink, as the one shown in Figure 1. In particular, we investigate the effect of rounding the corners of the rectangular channel cross section. Introducing the channel aspect ratio, β, and the non-dimensional smoothing radius, γ.

$$\beta = \frac{b}{a} \in [0,\,1],\, \gamma = \frac{2\,r}{b} \in [0,\,1] \tag{11}$$

the cross section perimeter, P, cross-sectional area, A_c, and hydraulic diameter, D_h, are equal to:

$$P = 2\,a\left[1+\beta-\frac{\beta\,\gamma}{2}(4-\pi)\right],\, A_c = a^2\left[\beta-\left(\frac{\beta\,\gamma}{2}\right)^2(4-\pi)\right],\, D_h = 2\,a\,\frac{\beta-\left(\frac{\beta\,\gamma}{2}\right)^2(4-\pi)}{1+\beta-\frac{\beta\,\gamma}{2}(4-\pi)}. \tag{12}$$

When changing the channel geometry, we must apply some restrictions. Following [20], we investigate the effect of changing the smoothing radius at fixed hydraulic diameter and aspect ratio on the heat transfer performances of the microchannel.

3.2. Application of PEC to electro-osmotic flow

As in electro-osmosis the fluid flow is driven by an applied external potential gradient across a microchannel, it is not possible a straightforward control of both the the mass flow rate and the pumping power. In fact, the mass flow rate of an EOF depends on several parameters such as: imposed electric field, electric potential at charged surface, ion concentration in the fluid, permittivity, channel cross section geometry. Thus, even changing the smoothing radius has an effect on the actual mass flowrate. Furthermore, Joule heating puts a limitation on the channel length, beyond which the solid surface is no longer cooled by the fluid. Therefore, straightforward application of PECs listed in Table 1 is not possible. As the channel length is given by external restrictions and the flow rate depends on channel geometry itself (that is what we aim to design), we will investigate two cases, which we simply refer to as FGa and FGb: maximizing the heat flux at fixed inlet temperature difference, FGa criterion; minimizing the inlet temperature difference at fixed heat flux, FGb criterion.

In order to apply the FGa and FGb criteria, we use Eq. (3) for calculation of heat flux q at fixed ΔT_i or inlet temperature difference ΔT_i at fixed q. When applying Eq. (3) to evaluate q or ΔT_i as a function of the smoothing radius, we first need to determine the actual mass flow rate, $\dot{m}$, the channel length, L, and the average convective heat transfer coefficient, $\overline{\alpha}$.

If the following non-dimensional parameters are fixed,

$$\Psi_0 = \frac{e\,z_i\,\zeta}{k_B\,T_w},\, k_D\,D_h = \sqrt{\frac{2\,e^2\,(c_0 N_A)\,z_i\,{D_h}^2}{\varepsilon\,k_B\,T_w}},\, E = \frac{E_x\,D_h}{\zeta}, \tag{13}$$

the non-dimensional bulk velocity $U_b = u_b/u_{eo}$, with $u_{eo} = \varepsilon\,\zeta\,E_x/\mu$, depends on the channel cross section geometry, in terms of channel aspect ratio $\beta = b/a$ and non-dimensional smoothing radius $\gamma = 2\,r/b$. Thus, the mass flow rate can be evaluated as $\dot{m} = \rho\,u_b A_c$. Once $\dot{m}$ is known, the pumping power, W, can be estimated as

$$W = \frac{\mu\,\dot{m}^2\,P\mathrm{Po}}{2\,(\rho\,A_c)^2}\,\frac{L}{D_h}, \tag{14}$$

where the Poiseuille number depends on both the aspect ratio and the non-dimensional smoothing radius, at fixed Ψ_0 and $k_D\,D_h$. As we have heat generation, critical length, l_{CR}, is defined at which the channel wall, at imposed temperature T_w, starts being heated by the fluid,

$$L_{cr}:\, \nabla T\cdot\hat{\mathbf{n}} = 0. \tag{15}$$

Considering longer channels would be detrimental in terms of heat transfer performance. At fixed Ψ_0, $k_D D_h$ and E, the non-dimensional critical length, defined as L_{cr}/D_h, depends on the channel geometry, in terms of β and γ, and on the non-dimensional Joule heating,

$$Q = \frac{\dot{q}_s {D_h}^2}{\lambda \Delta T_i} = \frac{\sigma \left(E_x D_h\right)^2}{\lambda \left(T_w - T_i\right)}. \tag{16}$$

Finally, the average heat transfer coefficient is evaluated via integration of the local Nusselt number along the channel length,

$$\overline{\alpha} = \frac{\overline{\mathrm{Nu}}\,\lambda}{D_h} = \frac{\lambda}{D_h} \int_0^{L_{cr}} \mathrm{Nu}\, dx. \tag{17}$$

Correlations for U_b and Po as a function of smoothing radius γ and for L_{cr} and $\overline{Nu}$ as a function of γ and non-dimensional source term Q have been developed from the numerical results provided in [24].
Here, we consider a single test case, which is defined by: wall temperature T_w (at which the fluid thermo-physical properties are estimated); ion concentration c_0 in the conduit fluid; fluid permittivity ε; electric field over channel axis E_x; Stern potential ζ at the Stern layer (close to the charged surface); channel hydraulic diameter D_h and aspect ratio β. Thus, the physical problem corresponds to a set of the non-dimensional parameters: Ψ_0, $k_D D_h$, E, defined in Eq. (13), and β. Following [24], we consider: $\Psi_0 = 2.92$, $k_D D_h = 8.45$, $E = 300$ and $\beta = 0.75$, while the non-dimensional heat source Q ranges between 10^{-3} and 10. As it is a good procedure to perform a non-dimensional analysis, we chose the sharp corner geometry as the reference configuration. At fixed problem parameters Ψ_0, $k_D D_h$, E and Q, we normalize the PEC objective functions, according to Eq. (4), with respect of the sharp corner configuration.

4. Result and discussion

4.1. Channel length, Nusselt number and Poiseuille number

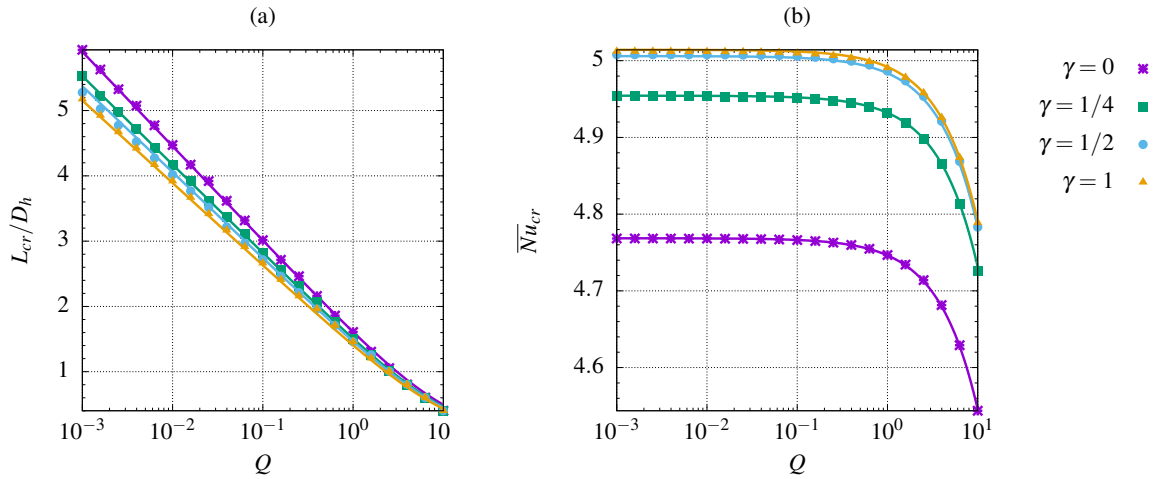

Figure 2. Numerical points from literature , [24], (markers) versus correlation (lines), Eqs. (18) and (19): critical length (a) and average Nusselt number (b) as a function of non-dimensional heat source and smoothing-radius. $\Psi_0 = 2.92$, $k_D D_h = 8.45$, $E = 300$, $\beta = 0.75$.

The numerical results from [24] are first used to correlate both the critical length L_{th} and the average

Nusselt number $\overline{\mathrm{Nu}}$ as a function of smoothing radius and non-dimensional heat source:

$$\frac{L_{cr}}{D_h} = (1.44687 - 0.18289\sqrt{\gamma})\log_{10}\left(1 + \frac{11.9618}{Q}\right), \tag{18}$$

$$\overline{Nu} = 5.01416 - 0.24559\,(1-\gamma)^{4.91061} - 0.022329\,Q. \tag{19}$$

Equation (18) is compared with numerical results in Figure 2(a), while Eq. (19) is compared with numerical results in Figure 2(b), showing good agreement. The critical length scales with the logarithm of the non-dimensional heat source, approaching infinite length for $Q \to 0$. The Nusselt number, averaged along L_{cr}, decreases with Q, and approaches the fully developed Nusselt number in case of negligible heat generation when $Q \to 0$.

The Poiseuille number Po and the non-dimensional bulk velocity U_b are correlated to the non-

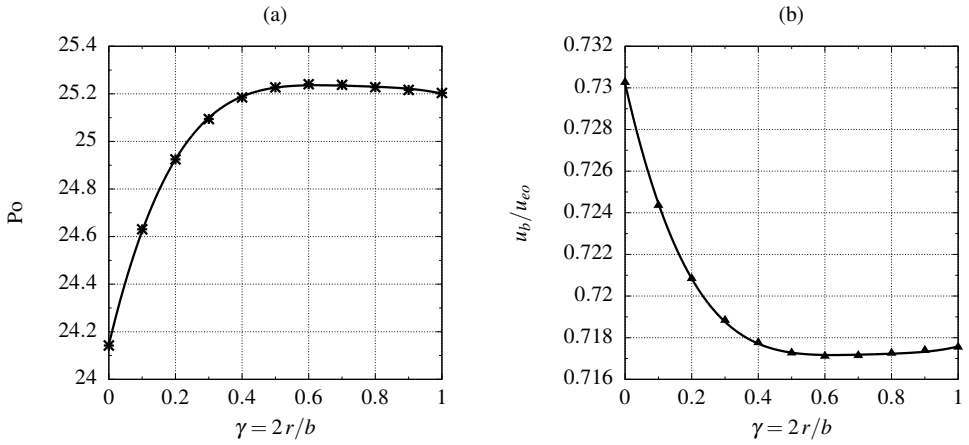

Figure 3. Numerical points from literature, [24], (markers) versus correlation (line): Poiseuille number (a) and non dimensional bulk velocity (b) of the hydrodynamically developed flow as a function of non-dimensional smoothing radius. $\Psi_0 = 2.92$, $k_D D_h = 8.45$.

dimensional smoothing radius via polynomial functions,

$$\mathrm{Po} = \sum_{n=0}^{4} a_n \gamma^n, U_b = \sum_{n=0}^{4} b_n \gamma^n \tag{20}$$

where coefficients a_n, b_n are listed in Table 2. Note that lower values of the Poiseuille number are

Table 2. Coefficient a_n, b_n of the polynomial fitting of Eq. (20).

a_0	24.1455	b_0	0.730217
a_1	5.84415	b_1	−0.0706503
a_2	−11.6856	b_2	0.142843
a_3	10.38	b_3	−0.128316
a_4	−3.48354	b_4	0.0434878

observed in the case of sharp corner configurtion, see Figure 3(a), due to local stagnation of the fluid near the channel corners. However, a local maximum of Po is reached at $\gamma \simeq 0.6$. An opposite behavior is observed for U_b, with the highest value corresponding to sharp corners ($\gamma = 0$) and a local minimum at $\gamma \simeq 0.6$. Eqs. (18), (19) and (20) are used to evaluate the critical channel length L_{cr}, the average heat transfer coefficient $\overline{\alpha}$ and the mass flow rate $\dot{m}$.

4.2. Application of PEC

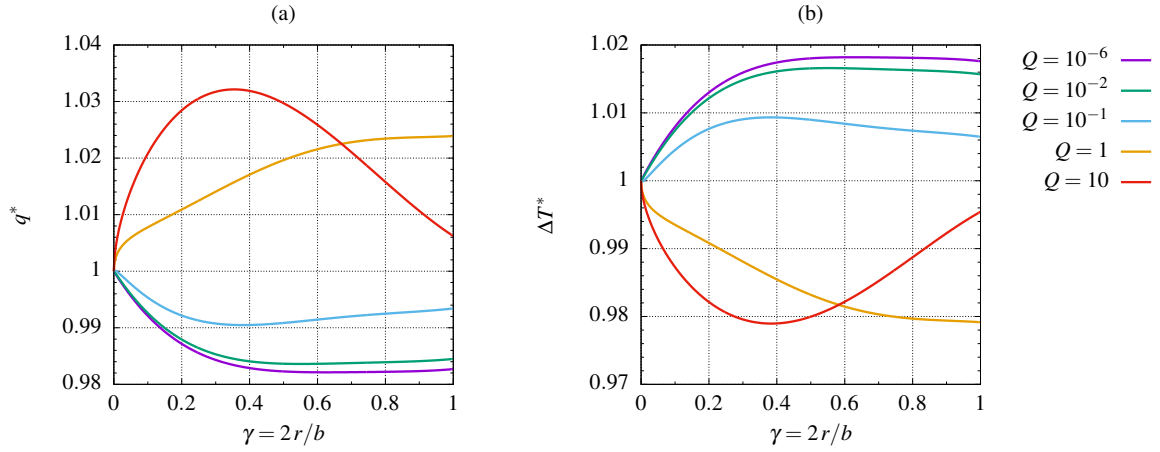

Figure 4. PEC objective function versus non-dimensional smoothing radius, at different non-dimensional heat source: heat flux at fixed inlet temperature difference, FGa (a); inlet temperature difference at fixed heat flux, FGb (b). $\Psi_0 = 2.92$, $k_D D_h = 8.45$, $E = 300$, $\beta = 0.75$.

Applying the geometrical constraint $D_h = \text{const}$ and estimating the mass flow rate as $\dot{m} = \rho\, u_b A_c$, with A_c depending on the smoothing radius according to Eq.(12) and bulk velocity $u_b = U_b\, u_{eo}$ given by Eq. (20), optimization via FGa and FGb criteria can be performed simply using Eq. (4). Objective functions are normalized to the sharp corner configuration, according to Eq. (4). The effect of changing the smoothing radius at different values of the non-dimensional heat generation Q, which is a parameter for the problem, is investigated. Figure 4(a) shows the heat flux as a function of the smoothing-radius (FGa criterion). The sharp corner configuration gives the maximum heat flux at negligible heat generation, while a local maximum at $\gamma \simeq 0.35$ is observed for $Q = 10$, which means high heat generation. Similar remarks can be made for the FGb criterion, see Figure 4(b), with the optimal configuration (i.e. minimum inlet temperature difference) corresponding to sharp corners in case of negligible heat generation, or $\gamma \simeq 0.4$ at $Q = 10$. It can be observed that the effect of heat generation on optimization process is negligible when $Q < 10^{-2}$. In fact, the average Nusselt number is unaffected by heat generation at low values of Q, while the non-dimensional critical length does not depend on Q at all, as $L_{cr} = f(\gamma) \times g(Q)$ according to Eq. (18) and, thus, $L_{cr}(\gamma)/L_{cr,0}$ is unaffected by Q. It is important to point out that at high Q the allowed channel length L_{cr} is too short to build an effective microchannel heat-sink, see Figure 2(a). However, extending results to lower values of Q ensures that longer channel are investigated, as L_{cr} grows at decreasing Q.
The variation of both the normalized mass flow rate and the normalized pumping power, evaluated via Eq. (14), are shown in Figure 5. Note that $\dot{m}^*$ and W^* do not depend on the heat generation term Q, which only appears in the governing energy equation, Eq. (9), and, thus, does not affect the flow field.

5. Conclusions

In this paper the transport phenomena occurring within a microchannel of rectangular cross-section with uniform wall temperature through which an electro-osmotic flow occurs were investigated, while considering the flow fully developed hydrodynamically but thermally developing (Graetz problem). The corners are then smoothed progressively and the effect of this change in the shape of the cross-section over the non-dimensional dissipated power or temperature difference between wall and fluid is investigated using the performance evaluation criteria introduced by Webb. Correlations are suggested for the Poiseuille and Nusselt numbers for all configurations as are criteria to obtain the maximum allowable - or critical - channel length, i.e. the length of the channel over which the walls start to

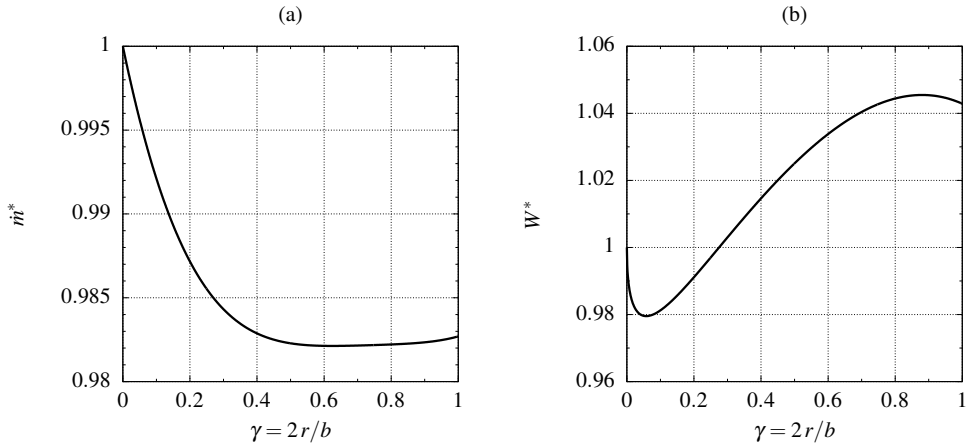

Figure 5. Mass flow rate (a) and pumping power (b) as a function of smoothin radius. $\Psi_0 = 2.92$, $k_D D_h = 8.45$, $E = 300$, $\beta = 0.75$.

cool the fluid, owing to Joule heating, in terms of the hydraulic diameter. Concerning the latter point, it is demonstrated that even an apparently insignificant amount of non-dimensional Joule heating shrinks the length of the channel dramatically: only for values of Q smaller than 10^{-6} does the critical channel length exceed ten hydraulic diameters. It is also appreciated that smoothing the radius has little influence on the non-dimensional critical channel length. It is demonstrated that there is an optimum radius of curvature to maximise the heat flux or minimise the temperature difference, when Q is significant, whilst the base configuration (sharp corners) has the best performance when Q is smaller. Pumping power also has both one minimum ($\gamma \approx 0.09$) and one maximum ($\gamma \approx 0.89$) with the non-dimensional radius of curvature.

References

[1] Kundu B and Saha S 2022 *Energies* **15**
[2] Hossan M, Dutta D, Islam N and Dutta P 2018 *Electrophoresis* **39** 702–731
[3] Kuznetsov V 2019 *Heat Transfer Engineering* **40** 711–724
[4] Morini G L, Lorenzini M, Colin S and Geoffroy S 2006 *Proceedings of the 4th International Conference on Nanochannels, Microchannels and Minichannels, ICNMM2006* vol 2006 A pp 411–418
[5] Yang Y, Chalabi H, Lorenzini M and Morini G L 2014 *Heat Transfer Engineering* **35** 159–170
[6] Keepaiboon C, Dalkilic A, Mahian O, Ahn H, Wongwises S, Mondal P and Shadloo M 2020 *Physics of Fluids* **32**
[7] Lorenzini M, Daprà I and Scarpi G 2017 *Applied Thermal Engineering* **122** 118–125
[8] Ohadi M, Choo K, Dessiatoun S and Cetegen E 2013 *Next Generation Microchannel Heat Exchangers* (NY: Springer)
[9] Han Y, Liu Y, Li M and Huang J 2012 A review of development of micro-channel heat exchanger applied in air-conditioning system *Energy Procedia* vol 14 pp 148–153
[10] Tuckerman D, Pease R, Guo Z, Hu J, Yildirim O, Deane G and Wood L 2011 Microchannel heat transfer: Early history, commercial applications, and emerging opportunities. *Proc. ASME 2011 9th ICNMM, Edmonton, AB, Canada* vol 2 p 739–756
[11] Kirby B 2010 *Micro- and Nanoscale Fluid Mechanics* (Cambridge, UK: Cambridge University Press)
[12] Al-Rjoub M, Roy A, Ganguli S and Banerjee R 2011 *International Journal of Heat and Mass Transfer* **54** 4560–4569
[13] Mala G, Li D, Werner C, Jacobasch H J and Ning Y 1997 *International Journal of Heat and Fluid Flow* **18** 489–496
[14] Wang C Y and Chang C C 2011 *Electrophoresis* **32** 1268–1272
[15] Geri M, Lorenzini M and Morini G 2012 *International Journal of Thermal Sciences* **55** 114–121
[16] Morini G L, Lorenzini M, Salvigni S and Spiga M 2005 Thermal performance of silicon micro heat-sinks with electrokinetically- driven flows *Proceedings of the 3rd International Conference on Microchannels and Minichannels, 2005* vol PART B pp 231–236
[17] Pramod K and Sen A 2014 *Journal of Electronic Packaging, Transactions of the ASME* **136** 03101201–03201214
[18] Ray S and Misra D 2010 *International Journal of Thermal Science* **49** 1763–1775
[19] Lorenzini M and Morini G L 2011 *Heat Transfer Engineering* **32** 1108–1116

[20] Lorenzini M and Suzzi N 2016 *Heat Transfer Engineering* **37** 1096–1104
[21] Lorenzini M 2020 *Journal of Thermal Science and Engineering Progress* **19** 100617
[22] Webb R L 1994 *Principle of Enhanced Heat Transfer* (Wiley, New York)
[23] Suzzi N and Lorenzini M 2019 *International Journal of Thermal Sciences* **145** 10603201–10603210
[24] Suzzi N and Lorenzini M 2021 *Fluids, MDPI* **6**
[25] Sadr R, Yoda M, Zheng Z and Conlisk T 2004 *Journal of Fluid Mechanics* **506** 357–367
[26] Webb R L 1981 *International Journal of Heat and Mass Transfer* **24** 715–726